Received: 4 July 2022 | Revised: 3 October 2022 | Accepted: 3 October 2022

DOI: 10.1111/joa.13780

Journal of Anatomy ANATOMICAL SOCIETY WILEY

BRIEF COMMUNICATION

Micro-CT analysis reveals the changes in bone mineral density in zebrafish craniofacial skeleton with age

Wei-Neng Liao[1] | May-Su You[2] | Zulvikar Syambani Ulhaq[3,4,5] | Jui-Ping Li[1] | Yun-Jin Jiang[2,6] | Jen-Kun Chen[1,6,7] | William Ka Fai Tse[3]

[1]Institute of Biomedical Engineering and Nanomedicine, National Health Research Institutes, Zhunan, Taiwan

[2]Institute of Molecular and Genomic Medicine, National Health Research Institutes, Zhunan, Taiwan

[3]Laboratory of Developmental Disorders and Toxicology, Center for Promotion of International Education and Research, Faculty of Agriculture, Kyushu University, Fukuoka, Japan

[4]National Research and Innovation Agency, Republic of Indonesia, Jakarta, Indonesia

[5]Department of Biochemistry, Maulana Malik Ibrahim State Islamic University, Malang, Indonesia

[6]Biotechnology Center, National Chung Hsing University, Taichung City, Taiwan

[7]Graduated Institute of Life Sciences, National Defense Medical Center, Taipei City, Taiwan

Correspondence
William Ka Fai Tse, Center for Promotion of International Education and Research, Faculty of Agriculture, Kyushu University, Fukuoka, Japan.
Email: kftse@agr.kyushu-u.ac.jp

Funding information
National Institute of Basic Biology, Japan, Grant/Award Number: 21-213 and 22NIBB322; Delta Electronics Inc., Grant/Award Number: C10-012; Education and Research Center for Mathematical and Data Science, Kyushu University, Japan, Grant/Award Number: 2022; Japan Society for the Promotion of Science, Japan, Grant/Award Number: 22K07025 and AJ179064; Ministry of Science and Technology, Taiwan, Grant/Award Number: 110-2740-B-400-001; National Health Research Institutes, Taiwan, Grant/Award Number: NHRI-BN-110-PP-31 and NHRI-MG-110-PP-08; Takeda Science Foundation, Japan, Grant/Award Number: 2020

Abstract

Bone has multiple functions in animals, such as supporting the body for mobility. The zebrafish skeleton is composed of craniofacial and axial skeletons. It shares a physiological curvature and consists of a similar number of vertebrae as humans. Bone degeneration and malformations have been widely studied in zebrafish as human disease models. High-resolution imaging and different bone properties such as density and volume can be obtained using micro-computed tomography (micro-CT). This study aimed to understand the possible changes in the structure and bone mineral density (BMD) of the vertebrae and craniofacial skeleton with age (4, 12 and 24 months post fertilisation [mpf]) in zebrafish. Our data showed that the BMD in the vertebrae and specific craniofacial skeleton (mandibular arch, ceratohyal and ethmoid plate) of 12 and 24 mpf fish were higher than that of the 4 mpf fish. In addition, we found the age-dependent increase in BMD was not ubiquitously observed in facial bones, and such differences were not correlated with bone type. In summary, such additional information on the craniofacial skeleton could help in understanding bone development throughout the lifespan of zebrafish.

KEYWORDS
bone density, bone type, fish head, imaging

1 | INTRODUCTION

Aging can be defined as the accumulation of deleterious changes over multiple levels of biological organisation, resulting in a decrease in whole-organism functionality with time (Weinert & Timiras, 2003). Various experimental models have been used to understand this mechanism. Zebrafish, a modern model organism, has been widely used in various research fields, such as toxicological studies and developmental biology. In addition, it has been used as a disease model because of its conserved pathological mechanisms and signalling pathways in humans. Its bone properties share many structural and phenotypic similarities with

humans, including the skeletal system (Schlegel & Stainier, 2007). Various studies have been conducted on aging in zebrafish, including physical and training abilities in aged zebrafish. A previous study showed that aged zebrafish have reduced training ability, swimming performance and routine swimming activity (Gilbert et al., 2014). More importantly, many aging features in humans are also found in zebrafish, such as degeneration of skeletal muscles (Short et al., 2005; Visser et al., 2005). To study disease development, it is important to investigate histology to identify disease status. Typical serial histology sectioning is widely used in research. However, this method introduces tissue loss and distortions that are required for tissue reconstruction (Arganda-Carreras et al., 2010). In addition, the limitation of section thickness has restricted its usage. To overcome these problems, micro-computed tomography (micro-CT) provides an alternative method. Micro-CT is commonly used to study hard mineralised tissues such as bones. Recent suggestions on the use of synchrotron hard X-rays in zebrafish have further pushed imaging to a higher resolution in the field (Ding et al., 2019). Because synchrotron imaging requires extensive hardware, the current majority of studies are still based on micro-CT.

A micro-CT study identified spinal deformity (or spinal curvature) in aged zebrafish (over 2-year-old) that is similar to human osteoarthritis (Hayes et al., 2014). Bone is a tissue with multiple functions in animals. It protects internal organs and acts as a site for haematogenesis and calcium homeostasis (Chan & Duque, 2002), besides providing the structure and support to the body for mobility. Recently, a study on trabecular bone in zebrafish showed that the bone volume reached its peak at 6 months and decreased afterwards (Monma et al., 2019). Spinal curvature has been widely studied for gene mutations and aging in zebrafish. However, information about the facial structure at different ages is limited. Various zebrafish studies on facial CT have been performed at particular time points to understand disease status, such as cleft palate. However, background information on facial bones at different ages is limited (Duncan et al., 2017; Li et al., 2022; Samuels et al., 2020). In this study, we applied micro-CT to investigate the possible BMD changes in the zebrafish vertebrae and craniofacial structure in three different ages (4, 12 and 24 months post fertilisation (mpf)) of zebrafish to fill this knowledge gap.

2 | MATERIALS AND METHODS

2.1 | Zebrafish

Wild-type female AB zebrafish (*Danieo rerio*) were used in this study. Five fish were used in each age group: 4 mpf (young), 12 mpf (adult) and 24 mpf (aging). These age groups are similar to those in a previous study that demonstrated detrimental sub-organismal effects of aging in zebrafish (Murtha et al., 2003). Zebrafish (AB strain, Zebrafish International Resource Center, Eugene, OR, USA) were kept at TZeTH (Zebrafish Core Facility at NHRI), where they were maintained in a water recirculating system at 28 °C on a 14 h light and 10 h dark cycle. Water quality (temperature at 27 ± 1°C, pH = 6.8–8.5, conductivity = 200–500 μS and dissolved oxygen ≥5 mg/ml) was monitored at all times. Fish were fed zebrafish powder food (Zeigler, Pentair Aquatic Eco-Systems, Inc.,) and Artemia (You et al., 2016) at least twice daily. Fish housing density was maximal at five fish per litre, following the AVMA guidelines. To minimise inbreeding, 10–20 pairs of fish were crossed to produce 80 randomly selected embryos for the next generation. The AB strain is the most popular strain used in facilities, particularly for embryo production. Extra feeding with a master-mix (enriched with vitamin D3 and minerals) is often applied. All animal procedures were approved by the Institutional Animal Care and Use Committee of the National Health Research Institutes (NHRI-IACUC-109036-A).

2.2 | Sample preparation for Micro-CT

Zebrafish were anaesthetised with 200 mg/L ethyl 3-aminobenzoate methanesulfonate and tricaine (MS222; Sigma) to collect the front end of the fish body at the following ages: 4, 12 and 24 mpf. Five fish from each age group were collected. At 20 min after the cessation of gill movements, five fish from each group were fixed by immersing in 40 ml of 4% paraformaldehyde (Electron Microscopy Sciences) in a 50 ml Falcon tube, incubated at 4°C for 24 h, and then embedded in 2% low melting agarose (Zymeset) in 2 ml Eppendorf tubes for micro-CT scanning.

2.3 | Micro-CT imaging and reconstruction

Micro-CT analysis was performed using a DELab μCT-100 (Delta Electronics Inc.). The voltage and current of the X-ray tube were 60 kVp and 500 μA, respectively, providing a 15 μm focal spot size and a maximum output power of 50 W. The 0.5 mm Al filter was applied to filter the X-rays. The flat-panel detector was a 14-bits CMOS detector with 1536 × 1944 pixels. In this study, the pixel size was 9 or 22.5 μm and the field of view (FOV) was 10 or 43 mm. Projection images were taken every 0.25° of sample rotation, which were reconstructed by the Feldkamp, Davis and Kress (FDK) analytical cone-beam reconstruction algorithm to generate each micro-CT image.

2.4 | Measurement, processing and analysis of bone mineral density (BMD)

Three-dimensional rendering and analysis, including registration of the head, precaudal vertebrae, caudal vertebrae and tail segments, were performed using the VIVID software (Gamma Medica-Ideas). For BMD measurements, a hydroxyapatite calibration curve was prepared from images of a micro-CT HA phantom (hydroxyapatite content: 0–1200 mg/cm^3; micro-CT HA D32, QRM GmbH), and all fish bone data were measured and analysed using DELab Image Analysis

(Delta Electrics, Inc.,). GraphPad Prism 5 (GraphPad Software, Inc.,) was used to plot bar charts to present the BMD of the precaudal vertebrae, caudal vertebrae, craniofacial bones and ethmoid plate in different groups of zebrafish. The Mann–Whitney U test was applied to compare BMD changes in zebrafish of different ages (4, 12 and 24 mpf) using IBM SPSS Statistics for Windows (Version 22.0. Armonk, NY: IBM Corp.) The *p*-values <0.05 and <0.01 denoted the presence of a statistically significant difference.

3 | RESULTS AND DISCUSSION

Zebrafish grow continuously with an increase in skeletal volume. The length of the fish is normally approximately 3–4 cm and can live for approximately 3 years (Gerhard, 2003). Numerous studies focusing on vertebrae have been performed to understand aging and spinal cord diseases. In addition, CT studies on the overall facial structure in zebrafish are not rare (Busse et al., 2020; Miyashita et al., 2020). However, to the best of our knowledge, no study has investigated the changes in craniofacial BMD during zebrafish growth. The study consisted of two parts: the first part focused on the vertebrae while the second part focused on the facial skeleton structure.

The zebrafish skeleton is composed of the craniofacial skeleton (parietal bones, jaw bones and opercles) and axial skeleton, including the vertebral column, ribs, intermuscular bones and fins (Dietrich et al., 2021). It shares a physiological curvature and consists of a similar number of vertebrae to humans (30–32 in zebrafish vs. 33 in humans). In this study, to obtain an overview of the fish condition, we first performed a full micro-CT scan of the fish (Figure 1a) and further investigated the possible changes in structure and BMD of the precaudal and caudal vertebrae of different ages. The zebrafish vertebral column is composed of Weberian apparatus, precaudal and caudal vertebrae and caudal fin vertebrae. The vertebral body centra is characterised by an hourglass shape. The precaudal vertebrae (orange region, Figure 1a) are the 10 vertebrae posterior to the Weberian vertebrae, while the caudal vertebrae (red region, Figure 1a) were located after the Weberian vertebrae. Precaudal vertebrae are composed of the centra, neural arches and spines, parapophyses and ribs. Caudal vertebrae are composed of the centra, neural arches, neural spines, haemal arches and haemal spines. Cross-sectional and sagittal images of the precaudal and caudal vertebrae are shown in Figure 1b. Regarding BMD, the quantified data suggested that this value increased with age (Figure 1c,d). The BMD of the precaudal vertebrae increased significantly from the 4 mpf fish ($0.140 \pm 0.008\,g/cm^3$) through 12 mpf ($0.449 \pm 0.019\,g/cm^3$) to the 24 mpf fish ($0.518 \pm 0.008\,g/cm^3$). Furthermore, the BMD of caudal vertebrae increased significantly from the 4 mpf fish ($0.125 \pm 0.018\,g/cm^3$) to 12 mpf ($0.354 \pm 0.017\,g/cm^3$), and was maintained in the 24 mpf fish ($0.381 \pm 0.024\,g/cm^3$). Based on BMD, loss of bone mineral was not observed. A previous report suggested an increase in BMD in the cortical bone and no change in the trabecular area after 6 mpf that could retain the strength of the vertebra (Monma et al., 2019). Moreover, almost all fish over 30 mpf show a common age-related spinal curvature (Hayes et al., 2014). However, we did not observe this in our facility. This phenomenon is subject to fish care and the nutritional status of the fish. The TZeTH is an Association for Assessment and Accreditation of Laboratory Animal Care International (AAALAC)-accredited facility since 2015, where fish health is regularly monitored and sufficient nutrition is provided. Therefore, good care may be a factor in maintaining fish BMD at 2 years of age (You et al., 2016).

In the second part of this study, we focused on the head. It should be noted that the zebrafish craniofacial skeleton is structurally more complex than that of most other vertebrates. The adult zebrafish skull is composed of 74 craniofacial bones, which is much higher than that of the mammalian skull which consists of 22 bones (Eames et al., 2013). Similar to mammals, the zebrafish skull is also composed of skeletal joints, including fibrous and articular joints in the jaw. In contrast, the craniofacial skeleton of zebrafish continues to grow throughout its lifetime (Bruneel & Witten, 2015). However, no study has reported the BMD of the facial bones of zebrafish at different ages. The micro-CT images (Figure 2) show heterogeneity of craniofacial structure in which the colour code indicates relatively high (red), medium (yellow-green) and low (blue) BMD (lateral view a–c; ventral view d–f; dorsal view g–i). The results clearly demonstrated that BMD increased with age and that this increase was substantial from 4 mpf ($0.116 \pm 0.007\,g/cm^3$) to 12 mpf ($0.421 \pm 0.025\,g/cm^3$). The difference in BMD values between 12 and 24 mpf fish (0.421 ± 0.025 vs. $0.539 \pm 0.083\,g/cm^3$) was much lower (Figure 2m). Specifically, we found that the highest BMD was observed in specific regions of the craniofacial skeleton in each experimental group. For example, in the 24 mpf fish, the highest BMD could be observed in the frontal (f) and parietal (pa) bone (dorsal view, Figure 2i); basioccipital (boc) bone (ventral view, Figure 2f); dentary (d) and quadrate (q) bone (lateral view, Figure 2c). In addition, frontier regions such as ethmoid (e) and kinethmoid (k) were also indicated as having high BMD (Figure 2e,f,h,i). Macroscopically, zebrafish facial bones can be classified into four types: acellular/cellular compact bones (white/blue), spongy bones, tubular bones (black) and chondroid bones (Figure 2j–l) (Weigele & Franz-Odendaal, 2016). We suggest that BMD is not directly related to bone type based on a comparison of CT images (Figure 2a–i) and bone types (Figure 2j–l).

We further studied the craniofacial skeleton in more detail and investigated BMD in the pharyngeal skeleton and ethmoid plates. The zebrafish pharyngeal skeleton can be divided into seven segments, including the mandibular arch (m), ceratohyal (c), ceratobranchial (cb) and branchial arches (ba) (Figure 3a–j). Among them, the mandibular arch and ceratohyal represent a relatively distinct structure and developmental pattern compared to ceratobranchial and the branchial arch (Figure 3d–f) (Schilling et al., 1996). The BMD of the mandibular arch (Figure 3k) increased significantly from the 4 mpf fish ($0.123 \pm 0.010\,g/cm^3$) through 12 mpf ($0.358 \pm 0.018\,g/cm^3$) to the 24 mpf fish ($0.437 \pm 0.053\,g/cm^3$). As for ceratohyal (Figure 3(k)), the BMD increased significantly from the 4 mpf fish ($0.099 \pm 0.010\,g/cm^3$) to 12 mpf ($0.313 \pm 0.027\,g/cm^3$) and was maintained in the 24 mpf fish ($0.334 \pm 0.025\,g/cm^3$). The mandibular arch consists of

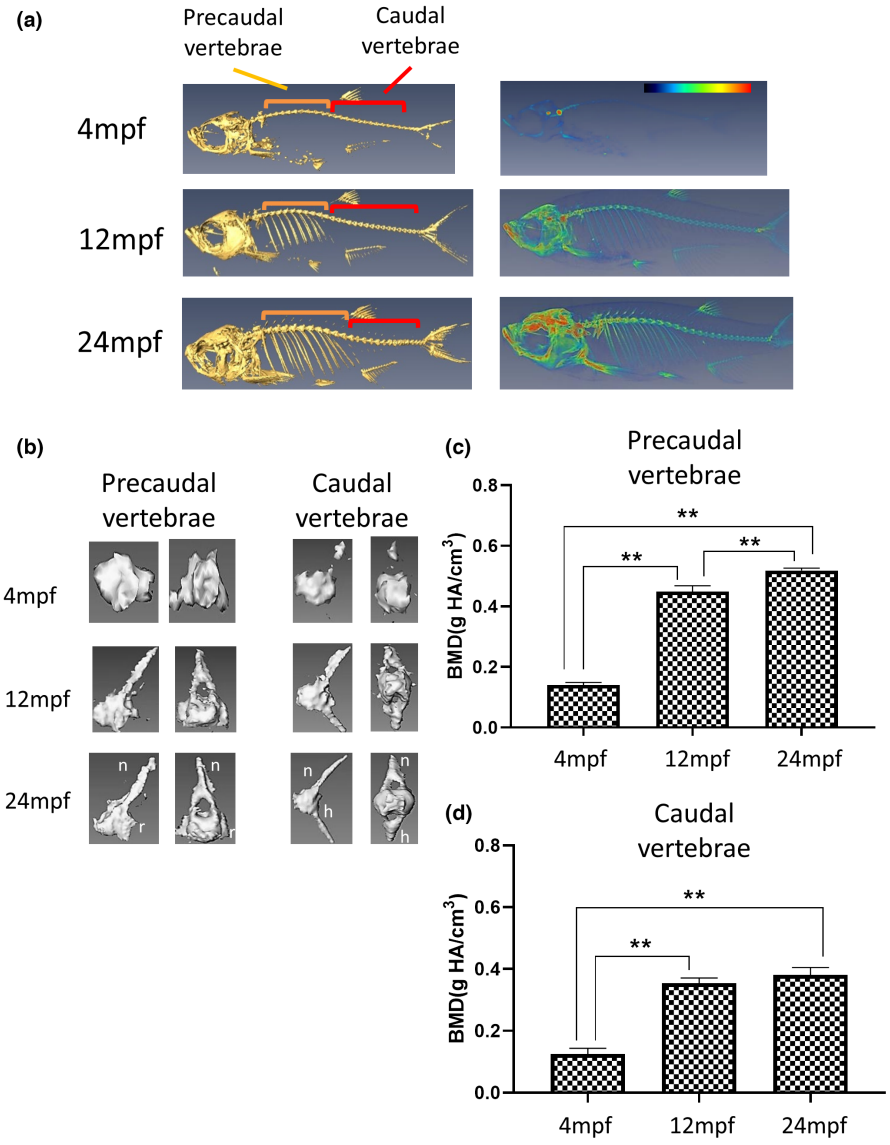

FIGURE 1 Micro-CT images and vertebral BMD of zebrafish at different ages. (a) Left panels show the full scan of the whole fish at the median plane. The orange regions mark the precaudal vertebrae, while the red indicate the caudal vertebrae. Right panels represent the converted heatmap of the micro-CT data. Red indicates the higher value of BMD, while blue refers to the low value of BMD. (b) Micro-CT image of the individual vertebra, both the median and the transverse plane. The left panel shows the precaudal vertebrae, with the neural arches (n) and ribs (r) labelled. The right panel displays the caudal vertebrae, featured with the haemal spines (h). (c) Quantified BMD value of precaudal vertebrae. (d) Quantified BMD value of caudal vertebrae. The vertebrae BMD increased from 4 mpf fish to 12 mpf and slightly increased or maintained in 24 mpf fish ($n = 5$). Statistically significant differences with p-value <0.01 were evaluated by the Mann–Whitney U test and are annotated with**.

dentary (d), anguloarticular (aa) and quadrate (q). Based on the bone types, d and aa are cellular compact bones; while q is the spongy bones that is the same as ceratohyal (c) (Kague et al., 2012). They develop from pharyngeal arches 1 and 2 (P1 and P2), whose formation is dependent on the migration of different groups of neural crest cells from rhombomeres and mesencephalons. One group of cranial neural crest cells (CNCCs) migrates ventrally to form P1 (Dougherty et al., 2013; Swartz et al., 2011), while other arches, including P2, are populated by different groups of CNCCs and surrounded by the mesoderm afterwards (Mork & Crump, 2015). The heatmap diagram in Figure 3a–c shows that it was likely that the spongy bones q and c had a higher BMD (red-orange colour) (Figure 3a–c) than others, and the overall quantified data (Figure 3k) showed significant BMD differences between the mandibular arch (d + aa + q) and ceratohyal (c) at different ages. In addition, we focused on the ethmoid plate, which is classified as a tubular bone (Figure 3g–i). Similar to the mandibular arch, the BMD of the ethmoid plate increased from 4 mpf ($0.101 \pm 0.011\,g/cm^3$) to 12 mpf ($0.290 \pm 0.036\,g/cm^3$) and further increased in strength up to 24 mpf ($0.435 \pm 0.120\,g/cm^3$) (Figure 3l). Taken together, the BMD of the mandibular arch, ceratohyal and ethmoid plate suggested that the bone type based on developmental origin was not the major factor correlating with BMD value.

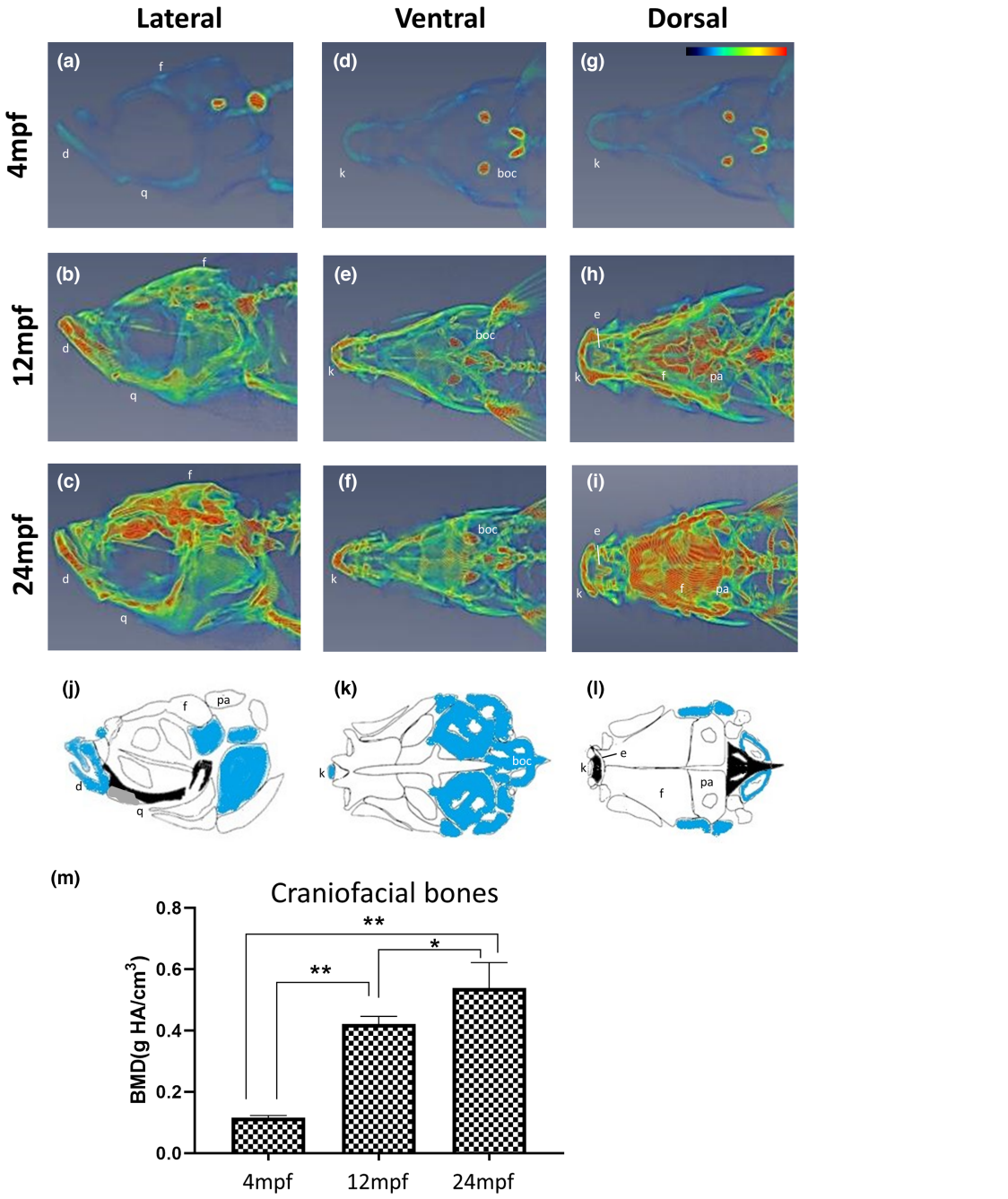

FIGURE 2 Micro-CT images and craniofacial BMD of zebrafish head at different ages. Data represent the converted heatmap of the micro-CT data focused on the zebrafish head in (a–c) lateral view, median plane; (d–f) ventral view, frontal plane; (g–i) dorsal view, frontal plane. Red indicates the higher value of BMD, while blue refers to the low value of BMD. (j–l) diagrams indicating the bone types in the zebrafish head: Acellular compact bones (white), cellular compact bones (blue), spongy bone (grey) and tubular bones (black) corresponding to the CT data. It should be noted that the base of the neurocranium was shown without the pharyngeal skeleton. Drawings were modified from (Kague et al., 2012). (m) Quantified BMD values of zebrafish skull. The craniofacial BMD increased from young fish to 12 mpf and slightly increased in the 24 mpf fish ($n = 5$). Statistically significant differences with p-value <0.05 and 0.01 were evaluated by the Mann–Whitney U test and annotated with * and ** respectively. boc, basioccipital; d, dentary; e, ethmoid; f, frontal; k, kinethmoid; pa, parietal; q, quadrate.

Vertebrae are the most well-studied skeletons for aging. It is well known that the BMD in trabecular and cortical decreases with age in humans. In contrast, zebrafish showed no alterations in trabecular BMD or increased cortical BMD. It has been suggested that this phenotype is unique to zebrafish (Monma et al., 2019). As craniofacial structure is not the primary research target to study aging, a limited number of reports have been published. Nevertheless, we have summarised the results of several human studies. A study on the BMD changes in the human skull at different ages and in the two sexes found that male skull BMD remained

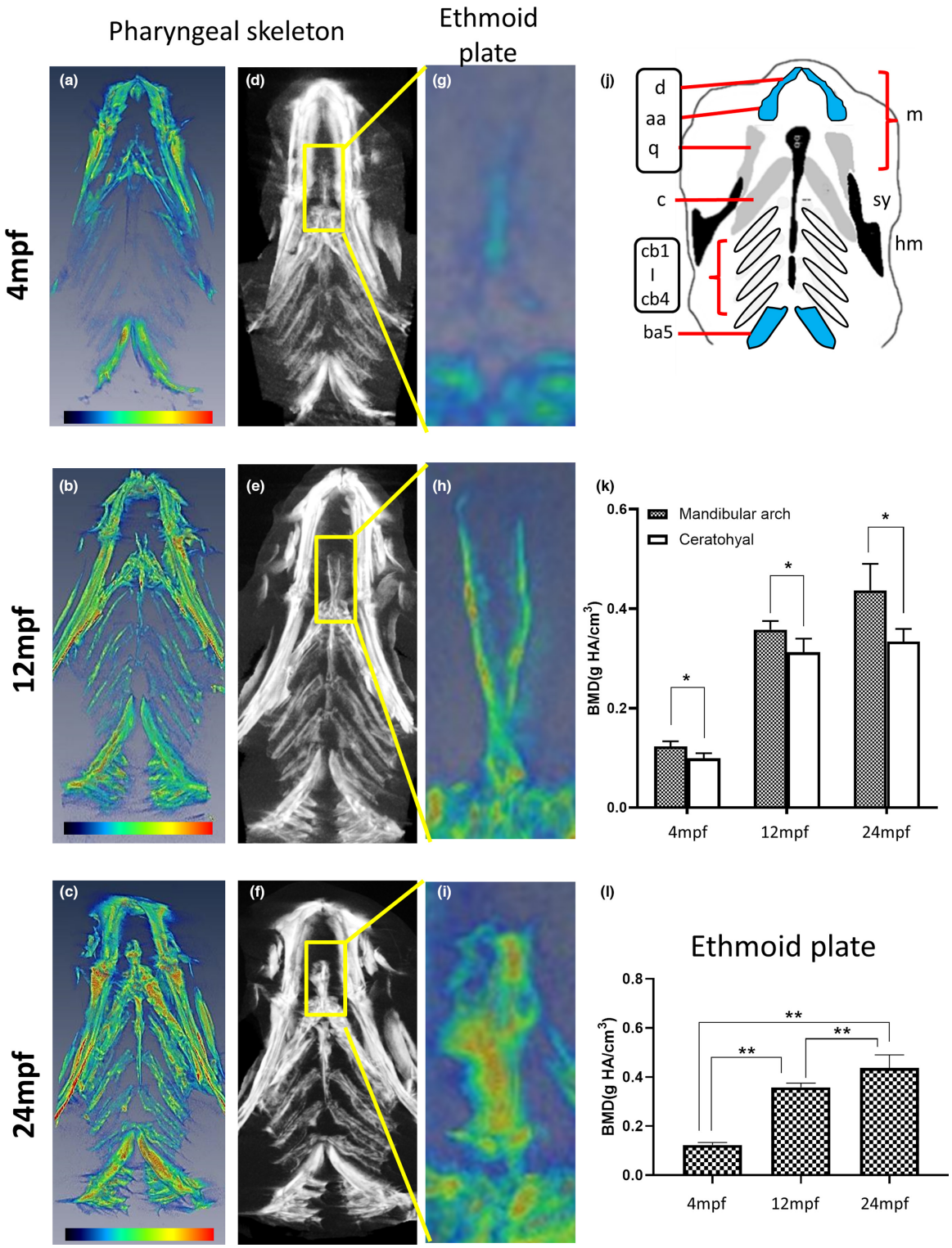

FIGURE 3 Micro-CT images and BMD of zebrafish pharyngeal skeleton and ethmoid plate at different ages. (a–c) Data represent the converted heatmap of the micro-CT data focused on the zebrafish pharyngeal skeleton. Red indicates the higher value of BMD, while blue refers to the low value of BMD. (d–f) Micro-CT images of the zebrafish pharyngeal skeleton from G to I show the enlarged ethmoid plate from the yellow box, frontal plane. (j) Diagram indicating the bone types in the zebrafish pharyngeal skeleton, ventral view: Acellular compact bones (white), cellular compact bones (blue), spongy bone (grey) and tubular bones (black) corresponding to the CT data. Drawings were modified from (Kague et al., 2012). (k) Quantified BMD values of mandibular arch and ceratohyal. Statistically significant differences with p-value <0.05 were evaluated by Wilcoxon signed-rank test and annotated with * as marked. (l) Quantified BMD values of the ethmoid plate. The BMD of ethmoid plate increased from 4 mpf fish to 12 mpf and increased further in the 24 mpf fish ($n = 5$). Statistically significant differences with p-value <0.01 were evaluated by the Mann–Whitney U test and annotated with ** as marked. aa, anguloarticular; ba5, branchial arch 5; c, ceratohyal; cb1-4, ceratobranchial 1–4; hm, hyomandibula; m, mandibular arch; q, quadrate; sy, sympleptic.

constant during lifetime, while females showed a slow reduction from 20 years onwards (Schulte-Geers et al., 2011). Another study focused on the younger group (0–20 years old) demonstrated that skull density increased rapidly until 3 years of age and continued to increase until adulthood (Delye et al., 2015). These studies were based on selected reference points in the skull. Studies on specific regions or bone types of the skull are limited. A previous study identified that the mandibular anterior region has the highest BMD, whereas the maxillary anterior and premolar regions have the lowest (Gulsahi et al., 2010). Similar to the vertebrae, the zebrafish craniofacial bones did not show a clear decrease in BMD in the old fish. A recent zebrafish study has shown that skeleton density increases with age up to 24 mpf, and this density changes with the body axis, with the highest density observed in the craniofacial skeleton (Nguyen et al., 2022). However, this study did not investigate the detailed density distribution in the head. To conclude, our current data are consistent with the available zebrafish studies and further suggest that BMD varies among different bone compartments and changes with age.

Zebrafish have been used as a model for craniofacial development and diseases (Duncan et al., 2017; Van Otterloo et al., 2016). Besides the general feature of zebrafish such as a well-known genome and simple transgenic tools, an open public online resource, FaceBase, could provide the researchers with a comprehensive structural database of faces (Eames et al., 2013; Samuels et al., 2020). This study provides additional background information on the BMD of the zebrafish craniofacial skeleton to fill the missing quantitative data on zebrafish of different ages. This work provides a general framework for advanced research using a craniofacial disease model.

AUTHOR CONTRIBUTIONS

WKFT conceived the ideas; WKFT, MSY, YJJ and JKC designed methodology; WNK and MSY investigated the study and collected the data; WNL and JKC analysed and visualised the data; ZSU and JPL contributed in revision; all authors contributed in writing the draft, revising the manuscript and gave final approval for publication.

ACKNOWLEDGEMENTS

The authors are grateful to have financial support from, National Health Research Institutes (NHRI-BN-110-PP-31 for JKC and NHRI-MG-110-PP-08 for YJJ) and partial financial support from Delta Electronics, Inc. (C10-012 for JKC). The biomedical researches in WKFT group are supported by the Japan Society for the Promotion of Science Grants-in-Aid for Scientific Research (22K07025); Bilateral Open Partnership Joint Research Project (AJ179064); the National Institute of Basic Biology Collaborative Research Program, Japan (21-213; 22NIBB322); Education and Research Center for Mathematical and Data Science, Kyushu University, Japan (2022). ZSU is supported by the Takeda Science Foundation's International Fellowship Program for Foreign Researchers (2020). We thank Chien-Ming Wang for handling/preparing zebrafish in the TZeTH (Zebrafish Core Facility at NHRI) (supported by grant from the Ministry of Science and Technology, Taiwan, MOST 110-2740-B-400-001 for YJJ and MSY).

DATA AVAILABILITY STATEMENT

Data sharing is not applicable to this article as no new data were created or analyzed in this study.

CONSENT FOR PUBLICATION

COI statement (from Jen-Kun Chen): The micro-CT (DELab μCT-100) used in this study was provided by Delta Electronics, Inc.

ORCID

Wei-Neng Liao https://orcid.org/0000-0002-1857-741X
Zulvikar Syambani Ulhaq https://orcid.org/0000-0002-2659-1940
Jui-Ping Li https://orcid.org/0000-0003-1868-5602
Yun-Jin Jiang https://orcid.org/0000-0003-0499-7306
Jen-Kun Chen https://orcid.org/0000-0002-3433-5971
William Ka Fai Tse https://orcid.org/0000-0002-3738-0460

REFERENCES

Arganda-Carreras, I., Fernández-González, R., Muñoz-Barrutia, A. & Ortiz-De-Solorzano, C. (2010) 3D reconstruction of histological sections: application to mammary gland tissue. *Microscopy Research and Technique*, 73, 1019–1029.

Bruneel, B. & Witten, P.E. (2015) Power and challenges of using zebrafish as a model for skeletal tissue imaging. *Connective Tissue Research*, 56, 161–173.

Busse, B., Galloway, J.L., Gray, R.S., Harris, M.P. & Kwon, R.Y. (2020) Zebrafish: an emerging model for orthopedic research. *Journal of Orthopaedic Research*, 38, 925–936.

Chan, G.K. & Duque, G. (2002) Age-related bone loss: old bone, new facts. *Gerontology*, 48, 62–71.

Delye, H., Clijmans, T., Mommaerts, M.Y., Sloten, J.V. & Goffin, J. (2015) Creating a normative database of age-specific 3D geometrical data, bone density, and bone thickness of the developing skull: a pilot study. *Journal of Neurosurgery. Pediatrics*, 16, 687–702.

Dietrich, K., Fiedler, I.A., Kurzyukova, A. et al. (2021) Skeletal biology and disease modeling in zebrafish. *Journal of Bone and Mineral Research*, 36, 436–458.

Ding, Y., Vanselow, D.J., Yakovlev, M.A., Katz, S.R., Lin, A.Y., Clark, D.P. et al. (2019) Computational 3D histological phenotyping of whole zebrafish by X-ray histotomography. *eLife*, 8.

Dougherty, M., Kamel, G., Grimaldi, M., Gfrerer, L., Shubinets, V., Ethier, R. et al. (2013) Distinct requirements for wnt9a and irf6 in extension and integration mechanisms during zebrafish palate morphogenesis. *Development*, 140, 76–81.

Duncan, K.M., Mukherjee, K., Cornell, R.A. & Liao, E.C. (2017) Zebrafish models of orofacial clefts. *Developmental Dynamics*, 246, 897–914.

Eames, B.F., DeLaurier, A., Ullmann, B., Huycke, T.R., Nichols, J.T., Dowd, J. et al. (2013) FishFace: interactive atlas of zebrafish craniofacial development at cellular resolution. *BMC Developmental Biology*, 13, 23.

Gerhard, G.S. (2003) Comparative aspects of zebrafish (Danio rerio) as a model for aging research. *Experimental Gerontology*, 38, 1333–1341.

Gilbert, M.J., Zerulla, T.C. & Tierney, K.B. (2014) Zebrafish (Danio rerio) as a model for the study of aging and exercise: physical ability and trainability decrease with age. *Experimental Gerontology*, 50, 106–113.

Gulsahi, A., Paksoy, C.S., Ozden, S., Kucuk, N.O., Cebeci, A.R. & Genc, Y. (2010) Assessment of bone mineral density in the jaws and its relationship to radiomorphometric indices. *Dento Maxillo Facial Radiology*, 39, 284–289.

Hayes, M., Gao, X., Yu, L.X., Paria, N., Henkelman, R.M., Wise, C.A. et al. (2014) ptk7 mutant zebrafish models of congenital and idiopathic

scoliosis implicate dysregulated Wnt signalling in disease. *Nature Communications*, 5, 4777.

Kague, E., Gallagher, M., Burke, S., Parsons, M., Franz-Odendaal, T. & Fisher, S. (2012) Skeletogenic fate of zebrafish cranial and trunk neural crest. *PLoS One*, 7, e47394.

Li, K., Fan, L., Tian, Y., Lou, S., Li, D., Ma, L. et al. (2022) Application of zebrafish in the study of craniomaxillofacial developmental anomalies. *Birth Defects Res*, 114, 583–595.

Miyashita, T., Baddam, P., Smeeton, J., Oel, A.P., Natarajan, N., Gordon, B. et al. (2020) nkx3.2 mutant zebrafish accommodate jaw joint loss through a phenocopy of the head shapes of Paleozoic jawless fish. *The Journal of Experimental Biology*, 223.

Monma, Y., Shimada, Y., Nakayama, H., Zang, L., Nishimura, N. & Tanaka, T. (2019) Aging-associated microstructural deterioration of vertebra in zebrafish. *Bone Reports*, 11, 100215.

Mork, L. & Crump, G. (2015) Zebrafish craniofacial development: a window into early patterning. *Current Topics in Developmental Biology*, 115, 235–269.

Murtha, J.M., Qi, W. & Keller, E.T. (2003) Hematologic and serum biochemical values for zebrafish (Danio rerio). *Comparative Medicine*, 53, 37–41.

Nguyen, S.V., Lanni, D., Xu, Y., Michaelson, J.S. & McMenamin, S.K. (2022) Dynamics of the zebrafish skeleton in three dimensions during juvenile and adult development. *Frontiers in Physiology*, 13, 875866.

Samuels, B.D., Aho, R., Brinkley, J.F., Bugacov, A., Feingold, E., Fisher, S. et al. (2020) FaceBase 3: analytical tools and FAIR resources for craniofacial and dental research. *Development (Cambridge, England)*, 147, dev191213.

Schilling, T.F., Piotrowski, T., Grandel, H., Brand, M., Heisenberg, C.P., Jiang, Y.J. et al. (1996) Jaw and branchial arch mutants in zebrafish I: branchial arches. *Development*, 123, 329–344.

Schlegel, A. & Stainier, D.Y. (2007) Lessons from "lower" organisms: what worms, flies, and zebrafish can teach us about human energy metabolism. *PLoS Genetics*, 3, e199.

Schulte-Geers, C., Obert, M., Schilling, R.L., Harth, S., Traupe, H., Gizewski, E.R. et al. (2011) Age and gender-dependent bone density changes of the human skull disclosed by high-resolution flat-panel computed tomography. *International Journal of Legal Medicine*, 125, 417–425.

Short, K.R., Bigelow, M.L., Kahl, J., Singh, R., Coenen-Schimke, J., Raghavakaimal, S. et al. (2005) Decline in skeletal muscle mitochondrial function with aging in humans. *Proceedings of the National Academy of Sciences of the United States of America*, 102, 5618–5623.

Swartz, M.E., Sheehan-Rooney, K., Dixon, M.J. & Eberhart, J.K. (2011) Examination of a palatogenic gene program in zebrafish. *Developmental Dynamics*, 240, 2204–2220.

Van Otterloo, E., Williams, T. & Artinger, K.B. (2016) The old and new face of craniofacial research: how animal models inform human craniofacial genetic and clinical data. *Developmental Biology*, 415, 171–187.

Visser, M., Goodpaster, B.H., Kritchevsky, S.B., Newman, A.B., Nevitt, M., Rubin, S.M. et al. (2005) Muscle mass, muscle strength, and muscle fat infiltration as predictors of incident mobility limitations in well-functioning older persons. *The Journals of Gerontology: Series A*, 60, 324–333.

Weigele, J. & Franz-Odendaal, T.A. (2016) Functional bone histology of zebrafish reveals two types of endochondral ossification, different types of osteoblast clusters and a new bone type. *Journal of Anatomy*, 229, 92–103.

Weinert, B.T. & Timiras, P.S. (2003) Invited review: theories of aging. *Journal of Applied Physiology*, 95, 1706–1716.

You, M.S., Jiang, Y.J., Yuh, C.H., Wang, C.M., Tang, C.H., Chuang, Y.J. et al. (2016) A sketch of the Taiwan zebrafish Core Facility. *Zebrafish*, 13(Suppl 1), S24–S29.

How to cite this article: Liao, W-N, You, M-S, Ulhaq, Z.S., Li, J-P, Jiang, Y-J & Chen, J-K. et al. (2023) Micro-CT analysis reveals the changes in bone mineral density in zebrafish craniofacial skeleton with age. *Journal of Anatomy*, 242, 544–551. Available from: https://doi.org/10.1111/joa.13780